Pancharatnam–Berry phase in space-variant polarization-state manipulations with subwavelength gratings

Ze'ev Bomzon, Vladimir Kleiner, and Erez Hasman

Optical Engineering Laboratory, Faculty of Mechanical Engineering, Technion—Israel Institute of Technology, Haifa 32000, Israel

Received March 19, 2001

We report the appearance of a geometrical phase in space-variant polarization-state manipulations. This phase is related to the classic Pancharatnam–Berry phase. We show a method with which to calculate it and experimentally demonstrate its effect, using subwavelength metal stripe space-variant gratings. The experiment is based on a unique grating for converting circularly polarized light at a wavelength of 10.6 μm into an azimuthally polarized beam. Our experimental evidence relies on analysis of far-field images of the resultant polarization. © 2001 Optical Society of America

OCIS codes: 260.5430, 050.1950, 350.3950, 050.2770, 350.1370, 230.5440.

The Pancharatnam–Berry phase is a well-known geometrical phase that appears when the polarization of a light beam is made to trace out a geodesic triangle on the Poincaré sphere.[1,2] The phases of the final and initial states differ by an amount equal to half of the solid angle encompassed by the triangle. Until now, most papers on the subject have treated the appearance of this phase in relation to propagating beams whose polarization is space invariant, (i.e., beams whose polarization is homogeneous over a transverse cross section). In typical experiments the polarization of the beam is altered by use of rotating wave plates and polarizers or by a wound optical fiber,[3,4] and the phase difference is introduced through the evolution of the beam in the time domain. However, to the best of our knowledge, no discussion has yet been made of the appearance of geometrical phases in space-variant (i.e., transversely inhomogeneous) polarization-state manipulations.[5] In this Letter we discuss geometrical phases introduced by such manipulations.

We show that, when a uniformly polarized beam undergoes space-variant polarization manipulation, its phase undergoes modification in the space domain. This phase modification is space varying and is of a geometrical nature. We provide a method for calculating this phase and provide experimental evidence to support our claims. The experimental support is based on a unique subwavelength metal stripe space-variant grating (SVG) designed for converting circularly polarized light into an azimuthally polarized beam. We demonstrate the existence of this phase by showing its effect on the far-field image of this beam, thereby emphasizing the relevance of correct phase determination in propagation of space-variant polarization beams.

Figure 1 illustrates space-variant polarization state manipulation by use of the Poincaré sphere. A beam initially in polarization state A undergoes space-variant manipulation, which results in a wave front with space-variant polarization; i.e., there exist points B_i $(i = 1, 2 \ldots)$ at which the local polarization is different. The local polarization ellipse at these points is defined by azimuthal angle ψ and by ellipticity $\tan \chi$, which are found from the Stokes parameters S_n $(n = 0, \ldots 3)$ as $\tan 2\psi = S_2/S_1$, $\sin 2\chi = S_3/S_0$.[6] Inasmuch as the change in polarization introduces a geometrical phase, we can expect space-variant polarization-state manipulation to introduce a space-variant phase modification. We consider such phenomena, which are due to SVGs.

SVGs are typically described by a grating vector:

$$\mathbf{K}_g(x, y) = [2\pi/\Lambda(x, y)]\{\cos[\beta(x, y)]\hat{x} + \sin[\beta(x, y)]\hat{y}\}, \tag{1}$$

where Λ is the period of the grating, $\hat{x}$ and $\hat{y}$ are unit vectors in the respective directions, and β is the direction of the vector, chosen such that it is directed perpendicular to the metal stripes. In a previous Letter[5] we showed a method for converting circularly polarized light into space-variant polarization by using SVGs. We showed that the transmitted polarization can be analyzed by use of a space-variant Jones matrix[6]:

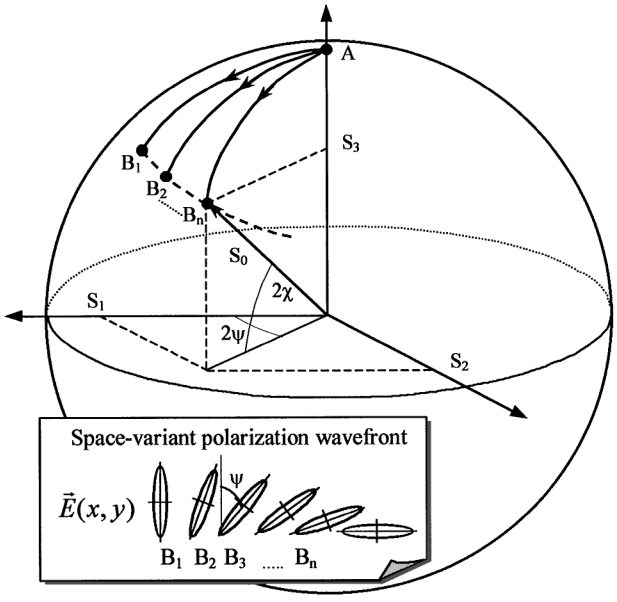

Fig. 1. Demonstration of space-variant polarization-state manipulations on a Poincaré sphere. Inset, resultant local polarization ellipse.

0146-9592/01/181424-03$15.00/0

$$J(x,y) = M[\beta(x,y)]J[\Lambda(x,y)]M^{-1}[\beta(x,y)], \qquad (2)$$

where $J[\Lambda(x,y)]$ is the Jones matrix that represents a SVG of period Λ with $\beta = 0$ and $M(\beta)$ is the 2×2 rotation matrix. Because the eigenpolarizations of the grating are oriented parallel and perpendicular to the grating vector, $J(\Lambda)$ is in general a diagonal matrix and can be written as

$$J(\Lambda) = \begin{bmatrix} p & o \\ o & q\exp(i\gamma) \end{bmatrix}\exp(i\varphi), \qquad (3)$$

where φ, which we associate with the dynamic phase of the grating, is chosen such that p, q, and γ are real. The elements of the matrix can be calculated by use of rigorous coupled-wave analysis,[7] and, once they have been calculated, the output polarization at any point of the grating is found as $\mathbf{E}_{\text{out}} = J(x,y)\mathbf{E}_A$, where $\mathbf{E}_A$ is the Jones vector of the incident polarization. To investigate the effect that such operators have on the phase of the transmitted beam, we assume circularly polarized light incident upon a SVG, i.e., $\mathbf{E}_A = (1, i)^T$. We assume two points, B_1 and B_2, for which the local period is equal and for which the angle between the grating vectors is θ. Because the period of the grating is equal at points B_1 and B_2, the polarization of $\mathbf{E}_{B_1}$ and $\mathbf{E}_{B_2}$ differs in azimuthal angle ($\psi_2 - \psi_1 = \theta$), whereas the ellipticity of $\tan\chi$ is equal at these points. Choosing the coordinate system such that the Jones matrix at point B_1 is diagonal, and using Eqs. (2) and (3), we find that

$$\mathbf{E}_{B_1} = \begin{bmatrix} p \\ iq\exp(i\gamma) \end{bmatrix}\exp(i\varphi),$$

$$\mathbf{E}_{B_2} = \begin{bmatrix} p\cos\theta + iq\exp(i\gamma)\sin\theta \\ -p\sin\theta + iq\exp(i\gamma)\cos\theta \end{bmatrix}\exp(i\varphi) \qquad (4)$$

and that the phase difference between them (the argument of their inner product[1,8]) is

$$\arg(\langle\mathbf{E}_{B_1}, \mathbf{E}_{B_2}\rangle) = \theta - \arctan\left[\frac{2pq\cos\gamma\sin\theta}{(p^2 + q^2)\cos\theta}\right]$$

$$= \theta - \arctan(\sin 2\chi\tan\theta), \qquad (5)$$

where $\sin 2\chi = S_3/S_0 = 2pq\cos\gamma/(p^2 + q^2)$.[6] Algebraic calculations show that this phase is exactly equal to half of the area of triangle AB_1B_2, thereby providing a meaningful connection to the Pancharatnam phase defined by this triangle.[8] Furthermore, as $J(\Lambda)$ is found by direct solution of the Maxwell equations, the dynamic and geometric phases associated with the change in period are already incorporated into the matrix, and therefore Eq. (2) permits calculation of the exact phase of the entire transmitted beam.

We can demonstrate the effect of this phase by considering a perfect space-variant polarizer for transforming circularly polarized light into azimuthal polarization, i.e., $\chi = 0$ and $\psi = \pi/2 + \theta$, where $\tan\theta = y/x$. On applying Eq. (5), we find that the output phase has been modified and that the beam can be described by the Jones vector

$$\begin{bmatrix} E_x(x,y) \\ E_y(x,y) \end{bmatrix} = i\exp(i\theta)\begin{pmatrix} -\sin\theta \\ \cos\theta \end{pmatrix}. \qquad (6)$$

Figure 2(a) describes the instantaneous real part of the electric field represented by this vector. Note that the intensity of the beam is uniform at all points; therefore the size and direction of the arrows in the figure indicate the phase. Furthermore, an illustration of the imaginary part of this vector will be rotated at 90° relative to Fig. 2(a). We see that the vectors at opposite sides of the center are in phase and are aimed in the same direction. We define this polarization as being in phase, as opposed to the antiphase polarization depicted in Fig. 2(b) into which no phase modification has been introduced. Although the beam is still azimuthally polarized, the vectors at opposite sides of the center are aimed in opposite directions and are antiphase. Although the two wave fronts described by Figs. 2(a) and 2(b) possess the same polarization, they consist of different phases, and it can be expected that they will propagate differently, producing distinguishable far-field images. For instance, symmetry dictates that the far field of Fig. 2(a) exhibit a peak at its center, whereas the far field of Fig. 2(b) should produce a dark center. Therefore it is possible to verify this phase by examining far-field images.

We constructed a SVG for converting circularly polarized light into an azimuthally polarized beam.[9] To do this, we required that grating direction β satisfy $\beta = \psi_{\text{desired}} - \Delta\psi(\Lambda)$, where ψ_{desired} is the desired azimuthal angle and $\Delta\psi(\Lambda)$ is the period-dependent angle between the large axis of the polarization ellipse and the grating vector. Note that the exact dependence of $\Delta\psi(\Lambda)$ on period is complicated and that it can be accurately calculated by rigorous coupled-wave analysis. Substituting β into Eq. (1) and requiring that $\nabla \times \mathbf{K}_g = 0$ results in a self-contained differential equation from which the grating vector is found. Finally, the grating function is found by integration of $\mathbf{K}_g$ along an arbitrary path to yield

$$\phi = \int \mathbf{K}_g d\mathbf{r} = \frac{2\pi r_0}{\Lambda_0}\cos[\Delta\psi(\Lambda_0)]$$

$$\times\left(\theta - \int^r \frac{\tan\{\Delta\psi[\Lambda(\mathbf{r})]\}}{r}dr\right), \qquad (7)$$

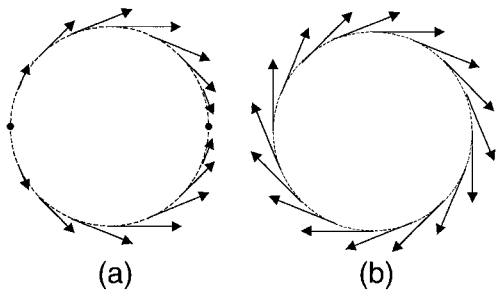

Fig. 2. Illustration of the instantaneous real part of the electric field vectors of in-phase and antiphase azimuthal polarization.

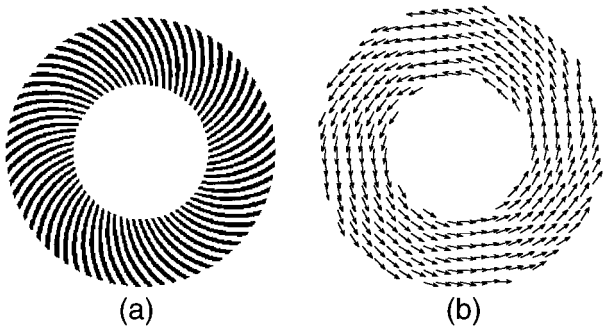

Fig. 3. (a) Magnified geometry of the grating for converting circular polarization into azimuthal polarization and (b) experimental measurement of the local azimuthal angle ψ.

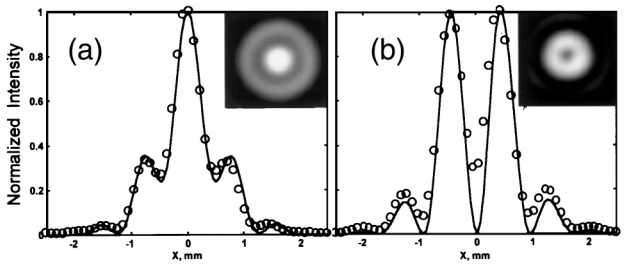

Fig. 4. Measured and calculated cross sections of the far-field images for (a) the in-phase and (b) the antiphase azimuthal polarization. Inset, experimental intensity distributions.

where r_0 and Λ_0 are constants and $\Lambda(r)$ is determined from the equation

$$K_0 = 2\pi/\Lambda(r) = (2\pi/\Lambda_0)\,(r_0 \cos[\Delta\psi(\Lambda_0)]/$$

$$r \cos\{\Delta\psi[\Lambda(r)]\})\,.$$

We realized a Lee-type binary grating[10] that describes the function in Eq. (7), with $\Lambda_0 = 2\ \mu$m and $r_0 = 4.8$ mm such that 2.5 mm $< r <$ 4.8 mm and 2 μm $< \Lambda <$ 3.2 μm. The metal stripes consisted of 10 of nm Ti and 60 of nm Au, which were deposited onto 500-μm-thick GaAs wafers by photolithography and a lift-off technique. The magnified geometry of this element is demonstrated in Fig. 3(a). After fabrication, an antireflective coating was applied to the back side of the element. We also realized a similar element for forming radial polarization. However, for this demonstration we address only the azimuthal beam.

We illuminated the grating with circularly polarized light at a wavelength of 10.6 μm from a CO_2 laser and then measured the Stokes parameters of the transmitted beam, using the four-measurement technique,[6] from which the local ellipticity and azimuthal angle were calculated at each point. Figure 3(b) shows the experimental azimuthal angle, ψ, of the output beam. The average experimental deviation ψ from ψ_{desired} was 5.5°, which we associate with a fabrication error. We also found an average ellipticity (tan χ) of 0.1, leading to an overall polarization purity (percent of energy in the desired direction) of 98.2%.

The transmitted beam should be in phase, as described by Eq. (6) and in Fig. 2(a). However, small deviations are expected because of the nonzero ellipticity and the deviation of ψ from ψ_{desired}. We used the Jones matrix formulation of Eq. (2) to calculate the beam accurately.

To determine the phase front of the transmitted beam, we observed the beam's far-field image. Figure 4(a) shows a calculated and a measured cross section for this image. We obtained the theoretical result by decomposing the beam into two orthogonal components with linear polarization, for which the far-field Fraunhoffer intensities were first calculated and then summed. We achieved the experimental result by focusing the beam through a lens with a 500-mm focal length. We found excellent agreement between theory and experiment, with the sharp peak at the center, clearly indicating that the beam is in phase. The beam can be converted into antiphase polarization by use of a spiral phase element (formed by 32-level reactive-ion etching of a ZnSe substrate), with a phase function $\exp[i\theta(x, y)]$.[11] Figure 4(b) shows the experimental and theoretical far-field images for this beam. A dark spot can be observed at the center of the far-field image, providing evidence that the beam is now antiphase and hence emphasizing the relevance of correct phase determination in polarization-state manipulation.

To conclude, we have shown the appearance of a geometrical phase in space-variant polarization-state manipulation. The determination of this phase is important in applications of polarization beam shaping such as atom trapping, optical tweezers, and tight focusing.[12]

Z. Bomzon's e-mail address is zbomzy@tx.technion.ac.il.

References

1. S. Pancharatnam, Proc. Ind. Acad. Sci. **44,** 247 (1956).
2. M. V. Berry, J. Mod. Opt. **34,** 1401 (1987).
3. R. Bhanderi and J. Samuel, Phys. Rev. Lett. **60,** 1211 (1988).
4. T. H. Chyba, L. J. Wang, L. Mandel, and R. Simon, Opt. Lett. **13,** 562 (1988).
5. Z. Bomzon, V. Kleiner, and E. Hasman, Opt. Lett. **26,** 33 (2000).
6. E. Collet, *Polarized Light* (Dekker, New York, 1993).
7. M. G. Moharam and T. K. Gaylord, J. Opt. Soc. Am. A **3,** 1780 (1986).
8. P. K. Aravind, Opt. Commun. **94,** 191 (1992).
9. Z. Bomzon, V. Kleiner, and E. Hasman, in *Conference on Lasers and Electro-Optics*, Vol. 56 of OSA Trends in Optics and Photonics Series (Optical Society of America, Washington, D.C., 2001), pp. 188–189.
10. W. H. Lee, Appl. Opt. **13,** 1677 (1974).
11. R. Oron, N. Davidson, A. A. Friesem, and E. Hasman, Opt. Lett. **25,** 939 (2000).
12. S. Quabis, R. Dorn, M. Eberler, O. Glöckl, and G. Leuchs, Opt. Commun. **179,** 1 (2000).